Multi-scale feature-feature interactions control patterns of hyporheic exchange in a simulated headwater mountain stream

Skuyler P. Herzog[1], Adam S. Ward[1], and Steven M. Wondzell[2]

[1] School of Public and Environmental Affairs, Indiana University, Bloomington, IN 47405, USA.

[2] Pacific Northwest Research Station, Forest Service, United States Department of Agriculture.

Corresponding author: Skuyler P. Herzog (skuyherz@iu.edu)

Key Points:

- Streambed topographic features of overlapping scales produced complex interactions and intermediate scale flowpaths in a mountain stream
- Intermediate scale features caused nearly complete hyporheic turnover by driving strong downwelling and truncating downvalley flows
- Upscaling efforts, field studies, and stream restoration should consider complex multi-scale interactions in steep mountain catchments

Index terms:
1830 Groundwater/surface water interaction
1825 Geomorphology: fluvial
1839 Hydrologic Scaling
1847 Modeling

Key words: hyporheic, multiscale modeling, river corridor, stream corridor, groundwater

Abstract

Recent predictions of hyporheic exchange at the basin-scale assume individual features control exchange independently of each other, which has been demonstrated in relatively uniform, low-gradient rivers. However, this assumption may not hold in steep catchments where both the type and size of individual features may vary over short distances, leading to irregular patterns of feature dominance on hyporheic exchange flows. Also, steep longitudinal gradients support substantial downvalley flows in the subsurface, which may create feedbacks between adjacent features. In this study we test the extent to which features interact with one another and whether they can be aggregated to make reach-scale predictions in a headwater mountain stream. Using systematic manipulations of a 2-D stream centerline model and spectral analyses, we test for the presence of both feature-feature and multi-scale interactions. Our results show that changing the height of individual step-pool features can alter hyporheic flow fields in neighboring, and sometimes distant, features. Spectral analyses revealed two scales of streambed topography – a local-scale of single features and an intermediate-scale that spanned multiple local-scale features. All features produced hyporheic exchange, but turnover of deeper hyporheic water only occurred at a few key locations where local- and intermediate-scale features reinforced each other. Further, shallow bedrock increases the ratio of local- and intermediate-scale flowpaths to regional-scale flowpaths. Conceptual models portraying hyporheic exchange as a series of nested flowpaths should include the interactions among streambed topographic features in mountain streams. These results have implications for upscaling, field experiments, and stream restoration in steep catchments.

Plain Language Summary

Many hyporheic studies have been done at scales of river reaches (100's of meters), but these are too costly to replicate across entire river basins. Instead, a current focus of hyporheic science is extrapolating reach-scale results with models that predict hyporheic flows across larger areas. These models assume that individual features are independent of one another and do not impact their neighbors. Using a model of a mountain stream reach, we manipulated individual features to test if and how much neighboring features affected one another. We also analyzed the streambed profile with a technique that breaks the topography into its component pieces, which may be difficult to observe in the field. First, we found that changing the height of a feature often influenced exchange flow through neighboring features, so the assumption of independence was not valid. Second, hyporheic exchange was predominantly shallow and associated with local-scale features, but deeper intermediate-scale hyporheic flows were also present and controlled by locations where larger-scale features amplified the effect of local-scale features. Our findings show that multi-scale feature-feature interactions can play an important role in steep streams, and these interactions need to be considered in upscaling models, field experiments, and stream restoration projects.

1. Introduction

Hyporheic exchange, which is important to many ecosystem services in the river corridor (Boulton et al., 1998; Brunke & Gonser, 1997; Stanford & Ward, 1988), depends on the organization and interaction of hydrologic forcing and geologic setting (Ward & Packman, 2019). Both sets of controls span several orders of magnitude, from baseflow to floods and from single bedforms to regional landforms, respectively (Tóth, 1963; Wörman et al., 2007). Here we adapt Tóth's terminology to the stream reach-scale, in which the local-scale refers to individual features (flows from a local topographic maximum to local minimum), intermediate-scale spans multiple local-scale features, and regional-scale flowpaths travel from the global maximum to the global minimum of the domain of interest. Of these scales, the local feature is the most widely studied (Boano et al., 2014; Ward, 2016). For example, many studies have demonstrated how local hyporheic flow fields vary with individual feature properties (e.g., height, hydraulic conductivity) (e.g., Hester & Doyle, 2008; Storey et al., 2003), variable stream discharge (Boano et al., 2007; Zimmer & Lautz, 2014), and ambient groundwater flows (Boano et al., 2008; Cardenas & Wilson, 2007; Fox et al., 2014). Recent work has expanded this continuum to show the relevance of smaller, sub-feature scales, including dead end pore space (e.g., Day-Lewis et al., 2017; Dehkordy et al., 2019), macrophyte roots (e.g., Nikolakopoulou et al., 2018), biofilms (e.g., Aubeneau et al., 2016; Caruso et al., 2017), and in-stream turbulence (Grant et al., 2018; e.g., Roche et al., 2018).

While many studies isolate a single feature or driver of hyporheic exchange, the interaction between controls at different scales is less commonly studied even though it is widely known that hyporheic exchange flows result from the superposition of all features and all scales (e.g., Tóth, 1963). In particular, the intermediate-scale that is larger than individual features but smaller than regional groundwater upwelling has rarely been studied (Wondzell, 2012) but is known to generate complex multi-feature flow cells (Robinson & Love, 2013; X.-S. Wang et al., 2017; Woessner, 2000). As a consequence, we have little understanding of how feature-to-feature interactions and the resulting intermediate flowpaths influence hyporheic exchange fluxes and transit timescales at the scale of river reaches to river basins. On a practical level, simplified multiscale models are needed to reliably predict multiscale connectivity, identify suitable sites and designs for stream restoration, and to inform management of water resources.

To-date, multiscale analysis of hyporheic exchange has primarily been in low-gradient stream reaches. For example, Stonedahl et al. (2013) found that the spatial scales of different feature classes (i.e., ripples, dunes, bars, and meanders) had distinct hyporheic exchange timescales, and that dunes were the single dominant scale. Each morphological feature class yielded unique exchange dynamics that interacted minimally with other scales. As a consequence, each scale could be characterized independently and recombined post-hoc to predict overall exchange dynamics in a study reach. In other words, there was no need to parameterize large-scale models with internal, multi-scale feedbacks and couplings. Once this relationship was proposed, the strategy was rapidly upscaled to the entire Mississippi basin, even distinguishing the importance of vertical versus lateral hyporheic exchanges in several sub-regions (Gomez-Velez et al., 2015) and estimating potential for denitrification (Kiel & Cardenas, 2014). Such predictive power is one of the primary goals of hyporheic science (Cardenas, 2015) and represents a major step forward. However, the technique was not designed for nor tested in high gradient (>4%) catchments with cascade or step-pool systems (Gomez-Velez & Harvey, 2014; Stonedahl et al., 2010). More work is needed to conceptualize and parameterize multi-scale interactions in steep headwater catchments, which exert outsized influence on downstream water quality and quantity (R. B. Alexander et al., 2007), and contribute drinking water to at least one third of the U.S. population (L. C. Alexander et al., 2018).

Modeling studies of lowland rivers largely neglect hydrostatic pressures, which are increasingly relevant in steeper mountain catchments (Wondzell & Gooseff, 2013). For example, hydrostatic forces were generally more dominant than hydrodynamic forces in streams with 0.2% to 5.3% gradients (Mojarrad et al., 2019). Mountain streams exceeding 10% slope skew further toward hydrostatic dominance and have increasingly large downvalley transport, or "underflow", within the subsurface (Castro & Hornberger, 1991; Kennedy et al., 1984; Ward, Gooseff, Voltz, et al., 2013). We hypothesize that as downvalley flow increases, the potential for interactions among individual features will also increase. This hypothesis is supported by a number of field and modeling studies that found evidence of complex interactions amongst features of the same or differing scales in mountain headwaters (Kasahara & Wondzell, 2003; Ward, Gooseff, & Singha, 2013; Wondzell & Swanson, 1996). Payn et al. (2009) observed strong evidence of intermediate flowpaths moving substantial amounts of water in steep (5.7-9.0%) Montana headwaters, which supports similar findings from a modeling study of a steep (~12%) headwater stream in the Oregon Cascades (Schmadel et al., 2017). In particular, Schmadel et al. (2017) found dozens of intermediate flowpaths spanning nearly the entire length of their ~300 m study reach, and that the timescales of these flowpaths (10-100 hrs) were relevant to biogeochemical processes like denitrification (Zarnetske et al., 2011). Interestingly, these flowpaths were not equally sensitive to changes in stream discharge and groundwater upwelling. Schmadel et al. (2017) raised the possibility that local streambed morphology controlled the sensitivity of these flowpaths across large ranges of discharge conditions, as steeper features have consistently larger hydraulic gradients to drive exchange flow than low-gradient features, regardless of discharge. This insensitivity of the shortest, near-stream flowpaths to changes in discharge is in good agreement with empirical observations and reduced complexity models in the same basin (Ward et al., 2017). Field and numerical studies agree that sensitive intermediate flowpaths tended to occur in less steep regions, but it was not clear if they were formed because of steep upstream features or the low gradient regions themselves, or if this was a spurious correlation based on the particular feature morphology and its position within the reach. This knowledge gap prevents simplified models from estimating reach-scale or larger transit time distributions in regions that have a significant fraction of intermediate flowpaths. Indeed, Payn et al. (2009) suggest that understanding the origin and terminus locations of intermediate flowpaths may be the key to predicting stream corridor connectivity and channel residence times.

Our objective in this study was to determine how the interactions between individual features control multi-scale hyporheic flowpaths in a study reach. Specifically, we ask (1) how sensitive are individual features and flowpaths to changes in morphology of other features in the reach (i.e., feature-feature interactions)? and (2) are multiple scales of controls present that can be decomposed and reconstructed additively, as in Stonedahl et al. (2013)? Using a 2-D numerical model, we systematically varied the heights of individual features and quantified the resulting changes in hyporheic flowpaths across multiple scales. We also used spectral analysis of the streambed profile to test for the presence of larger-scale topography. Together, these analyses tested our hypothesis that interactions among features are critically important in steep mountain streams and influence hyporheic exchange at multiple scales. If present, these coupled multi-scale feedbacks would need to be included in upscaling efforts for mountain stream networks.

2. Methods

2.1 Mathematical modeling of hyporheic flowpaths

The basecase model for this study is identical to that of Schmadel et al. (2017) and Ward et al. (2018b). In brief, the model is a two-dimensional, finite element model constructed in COMSOL Multiphysics and represents a profile along the stream centerline of Watershed 1 (WS01), a steep (~12%) second order mountain watershed in the H.J. Andrews Experimental Forest (HJA) in Oregon, USA. It is a heuristic model meant to provide a conceptual yet realistic representation of hyporheic flow in steep, constrained mountain catchments with step-pool morphology. The domain geometry was based on surveyed streambed topography and an average 3-m depth to bedrock in 2nd order streams of the HJA (after Gooseff et al., 2006), offset from a linear best-fit to the streambed topography. The upstream, bottom, and downstream boundaries of the model domain were set to no flow, consistent with a reach underlain by low permeability bedrock and bookended by visible bedrock outcrops. Surface water was imposed as a constant head boundary and parameterized by surveyed surface water elevations. Here we considered the 3 m deep and 300 m long lower reach (90-390 m above the stream gauge), medium discharge (7 L s^{-1}) scenario described by Schmadel et al. (2017). No other discharge scenarios were used, as Schmadel et al. (2017) and Ward et al. (2018b) concluded that discharge was not a primary control on hyporheic flow in WS01 as long as the streambed was saturated. That is, increasing stage with rising discharge had negligible effects on the slope of the hydraulic grade line such that most hyporheic flowpaths did not change significantly in their geometry nor transit times. At this discharge the subsurface domain was completely saturated, so subsurface flow was modeled using Darcy's Law with porosity set to 0.2 and a hydraulic conductivity of 7×10^{-5} m s^{-1}, both based on reported values for poorly-sorted colluvium at this site (Wondzell et al., 2009). For further detail on WS01, the reader is referred to Wondzell (2006) and Voltz et al. (2013).

2.2 Model assumptions

Schmadel et al. (2017) studied the impact of three discharge scenarios and groundwater upwelling on hyporheic exchange in a steep mountain stream. Building on that study, Ward et al. (2018b) simulated hyporheic flows in the same reach across an entire annual hydrologic cycle. By adopting the basecase model from these two studies we leverage their prior investigations alongside our new systematic manipulations of streambed topography. The consistent modeling methodology allows us to comment on the relative role of hydrologic forcing in comparison to geologic setting, as the former would otherwise be beyond the scope of our current study. Accordingly, we carry forward the key assumptions and limitations of the prior study, summarized below.

Topographic survey points of the stream thalweg, which are the basis of the model domain top boundary, were selected to capture local topographic highs and lows associated with the dominant step-pool morphology of the system. The median longitudinal and vertical distances between survey points of were 0.8 m and 0.12 m, respectively, but measurements were made more frequently in high relief areas to characterize the dominant morphology of the system as observed during the survey (Schmadel et al., 2017). This study considered the dominant local features such as steps and pools, and any larger-scale patterns that may be present along the reach. Bedrock was not visible in the reach except at the upstream and downstream model boundaries, so steps represent logs, boulders, or debris jams that accumulate sediment wedges behind them. In comparison to low-gradient studies, smaller-scale features bedforms such as ripples were not present in our study reach, which has an armored cobble bed. Other fine-scale topographic features such as cobbles and grain clusters were not distinguished from the general topography. We also omitted lateral exchange that might arise due to meanders or alternate bars given the 2-D domain used for our simulation.

In our analysis of feature-scale and larger hyporheic flow geometries, we assume hydrostatic forces are dominant over hydrodynamic pressures in our mountain headwater stream (Wondzell and Gooseff, 2013). Hydrodynamic forces may be important drivers of hyporheic exchange in low gradient systems and can reduce the hydrostatic head experienced at the sediment water interface (Bao et al., 2018; Sickbert & Peterson, 2014). However, we assme hydrodynamically drive exchange is negligible in our steep step-pool streams due to low surface water velocities and dominant downvalley hydrostatic gradients (Wondzell & Gooseff, 2013). Therefore we neglect hydrodynamic processes to reduce computational demand, consistent with many hyporheic exchange models of mountain streams (citations). We also do not consider heterogeneities in subsurface architecture (e.g., bedrock topography, hydraulic conductivity), which are known to influence hyporheic exchange (Bao et al., 2018; Pryshlak et al., 2015; Vaux, 1968; Ward et al., 2011) but poorly constrained, requiring a vastly expanded sensitivity analysis that is beyond our scope.

2.3 Classification and manipulations of individual local-scale features

Step-pools in the field survey did not present idealized, uniform features with a single, clear crest, making it difficult to isolate individual features. Consequently, we classified individual features according to up- and downwelling zones at the sediment-water interface rather than from the surface topography. In other words, the boundaries of each local-scale feature were defined by the contiguous hyporheic flow cells beneath them (after Gooseff et al., 2003). Upwelling zones were defined by streambed locations where the simulated Darcy flux was upward, while downwelling zones were the locations where water flowed into the hyporheic domain. Our model was not designed to represent sub-feature-scale flows, so any upwelling or downwelling zone that was less than half the median survey distance (i.e., <0.4 m) was ignored and incorporated into the surrounding downwelling or upwelling zone, respectively. This prevented small heterogeneities from artificially fracturing large features, as the survey points were based on visual identification of relevant, feature-scale surface topography. Starting from the downstream end of the model, each contiguous upwelling zone was paired with its upstream, adjacent downwelling zone to define a hyporheic flow cell, as in Gooseff et al. (2003). The basecase model resulted in 66 discrete flow cells, each of which was classified as a single, local-scale feature. Flows that downwelled at one feature but surfaced in another were considered intermediate-scale, whereas flows that spanned the entire model domain were classified as regional-scale. For context, typical flowpaths lengths were < 10 m for local-scale, 10-290 m for intermediate-scale, and 300 m for regional-scale in our model domain.

We tested the sensitivity of all hyporheic flowpaths to each feature's geometry by systematically scaling each feature in the vertical dimension by ±10, ±25, and ±50% (six separate simulations per feature), modifying one feature at a time. These manipulations are analogous to – and qualitatively similar to – common natural depositional and erosive processes (e.g., episodic accumulation and degradation of logs and debris), albeit simplified for this conceptual analysis. We did not modify the 3 features closest to the downstream and upstream boundaries, taking them as conditioning model inflows and outflows, resulting in n = 60 features that were modified. We conducted a total of 361 simulations (60 features × 6 scenarios each, plus 1 basecase model). We stretched features vertically to increase their heights and slopes without altering their spacing (Figure S1). Hereafter, we call the feature being manipulated the "focal" feature. Within the focal feature, the vertical offsets between adjacent points were stretched by a multiplier according to the specific scenario (e.g., a multiplier of 1.5 for +50% scenario). For each manipulation, the original start and endpoints of the focal feature were held constant, so that there was no change in domain geometry except at the focal feature. In many cases features switched from concave at basecase to convex in the -25% and -50% scenarios, but this approach was necessary to maintain the same overall gradient and sediment depths throughout the rest of the model domain. The hydraulic head boundary was also adjusted slightly at each modified feature to preserve the original stream depth (i.e., the offset between the sediment-water interface and water level). Although the stream depth might change in response to altered topography in the field, far greater changes in depth did not significantly alter hyporheic flow geometries in prior modeling investigations of this same reach (Schmadel et al., 2017; Ward et al., 2018b). In cases where the modified water level exceeded the upstream water level, the modified water level was projected upstream as a pool until it intersected with the surveyed upstream water surface. Models averaged approximately 127,000 triangular mesh elements, each ranging between 0.05-0.12 m in height, and all elements had quality of at least 0.73.

As in Schmadel et al. (2017), particles were released at the streambed every 10 cm and tracked until they exited the subsurface domain. For each simulation, particle traces were exported and used to calculate flowpath lengths, transit times, and geometries. We released 3,013 particles per simulation, totaling more than 1 million particles for this study. To evaluate which flowpaths changed significantly between scenarios, Schmadel et al. (2017) used a threshold of 5% change in flowpath residence time. We used the same 5% cutoff, but focus on flowpath length rather than timescale because our interests are in the spatial patterns of flowpaths whereas Schmadel et al. (2017) were focused on transit times. Analyses by Schmadel et al. (2017), and our own simulations, showed that residence times were tightly correlated with flowpath lengths (R^2 = 0.997) due to homogeneous, isotropic subsurface parameterization in our model. Percent change could only be calculated for particles that downwelled in the basecase model (i.e., nonzero flowpath length), but we also tracked newly activated flowpaths (i.e., particles released in locations that upwelled in the basecase model but downwelled in subsequent scenarios) and when flowpaths changed scales, such as from local (within a single feature) to intermediate (spanning multiple local features) or vice-versa. In contrast to studies with multiple realizations of equally likely scenarios, our manipulations were designed to systematically test the sensitivity of all hyporheic flowpaths in the reach to changes in the height of each focal feature. It is likely that some flowpaths only change significantly with proximal or extreme (±50%) manipulations, and not as a result of distant and/or small (±10%) alterations. For this reason, we considered both the average and extreme behaviors of each flowpath to determine patterns of sensitivity.

2.4 Quantification of multiple topographic scales

In addition to modifying features and testing their impact, the basecase topography was analyzed using the periodogram function in MATLAB and the MATLAB Curve Fitting Tool, both based on the Fast Fourier Transform technique. Notably, these analyses did not define any separate scales a priori. Rather, the analyses are designed to find all dominant wavelengths present in the study reach. For topographic analyses, the surveyed streambed topography was detrended and interpolated to generate an even 0.1 m spacing between points in accordance with standard practice (Trauth, 2015). The Curve Fitting Tool represented the topography as a summation of up to 8 sine waves, using R^2, SSE, and RMSE as objective functions to determine the optimal fits. We compared the different topographic scales identified by these analyses to see if they could be easily separated as in Stonedahl et al. (2013).

3. Results

3.1 The flowpaths near the centers of hyporheic flow cells are more consistent than distal flowpaths

In the basecase simulation 56% of the streambed was downwelling whereas 44% was upwelling, but the total upwelling and downwelling fluxes were equal within reasonable numerical error (net boundary flux equivalent to -0.1 mL s^{-1} per meter of streambed). These patterns were sensitive to changes in topography, as 60% of the streambed switched between upwelling and downwelling in at least one of the 360 simulations we analyzed. Note, however, that in any single simulation, only a small number of flowpaths would switch between upwelling and downwelling. We found 22% of the streambed always downwelled and 18% always upwelled, demonstrating that flowpaths are not uniformly sensitive to changes in topography. The total amount of hyporheic exchange flux in the reach was insensitive to manipulations of individual features: the range in reach-scale flux values was only ~5% of the mean value, and we do not further discuss exchange flux for this reason. In terms of scale, 73% of downwelling particles stayed in local flow cells in the basecase model, while 27% traveled along intermediate flows involving multiple features. Regional flowpaths were negligible in the basecase model and across all simulations; only a small subset of particles that downwelled in the first meter of the model domain traveled to the end of the model as downvalley flow. The majority of particles were consistent in scale across the simulations: 42% never changed scales (i.e., from local-to-intermediate or vice versa) and a further 49% changed scales in 6 or less manipulations (i.e., the number of manipulations for each focal feature; Figure S2). Instead, the locations of local and intermediate-scale flowpaths were remarkably consistent, yielding a discrete set of streambed locations that initiated intermediate-scale flows across nearly all simulations. The features associated with intermediate flowpaths locations were not noticeably taller or steeper than the other features (Figure S3).

We assessed individual flowpath lengths in addition to overall trends in flow directions and scale. We found that 96% of the downwelling flowpaths changed by more than 5% in length in at least one of the 360 manipulations, but changes were not consistent between different simulations. On average, only 2% of the flowpath lengths changed significantly in response to any individual manipulation and no flowpaths were sensitive to change in every single manipulation. In fact, more than 90% of particles changed significantly in <10% of simulations and the most sensitive particle changed significantly in approximately two-thirds of all model runs. Taken together, these results show that almost all flowpaths experienced significant changes in at least one simulation but were insensitive to the majority of manipulations. These results match our expectation that most particles would be sensitive to large (±50%) and nearby changes but not to more distant and minor (±10%) changes.

Next, we evaluated whether spatial location influenced flowpath sensitivity. Visual inspection of particle traces (e.g., Figure 1a) show that flowpath geometries in the center of each local hyporheic flow cell (i.e., near the inflection point between downwelling and upwelling zones – typically the crest of a step) were the most stable, changing very little regardless of the topographic manipulations to the focal feature or neighboring features. However, these short central flowpaths were actually slightly more likely to have significant changes in length compared to more distal flowpaths (Figure S4) because even very small changes can still represent >5% of the basecase flowpath length for central flowpaths. Despite the greater likelihood of changing by >5% in length, the central flowpaths were far less likely than more distal flowpaths to change scale. Significant changes in flowpaths further from the center of a focal feature translated into much greater changes in absolute length, which were sometimes large enough to span neighboring features (i.e., switching from local upwelling within the flow cell of the focal feature to upwelling in a more distant feature; Fig. 1b). That is, the more distal a flowpath is from the central inflection point, the more likely it is to be intermediate-scale. Across all features (n=60), the most central flowpaths (<1 m from the feature inflection points) remained local-scale in >99.9% of manipulations with few intermediate-scale outliers (red crosshairs in Fig. 1b). In Figure 1b, this most central region is so consistent that boxplots and outliers can hardly be distinguished from the 100% local-scale line. Moving outward, particles released in the downwelling zone 1-2 m upstream from the center of features were still local on average, but an increasing number of outliers visible near the 0% local-scale line show a greater propensity to become intermediate-scale flowpaths. Finally, flowpaths >2 m upstream of the center of each focal feature became more variable. The interquartile range of these more distal flowpaths spans from ~5-100% local-scale, showing that flowpaths at that distance are almost always local in some features, but almost always intermediate in others. Thus, the distal edges are more sensitive than the central areas to changes in focal feature height. The distal edges of local features were not only the beginning of most intermediate-scale flowpaths, they were also commonly the terminus locations. For example, particles that switched to intermediate flow could upwell at a range of downstream locations, but these locations were discrete segments rather than one continuous zone, because intermediate flowpaths must also upwell in the more variable regions between local features (Fig 1a).

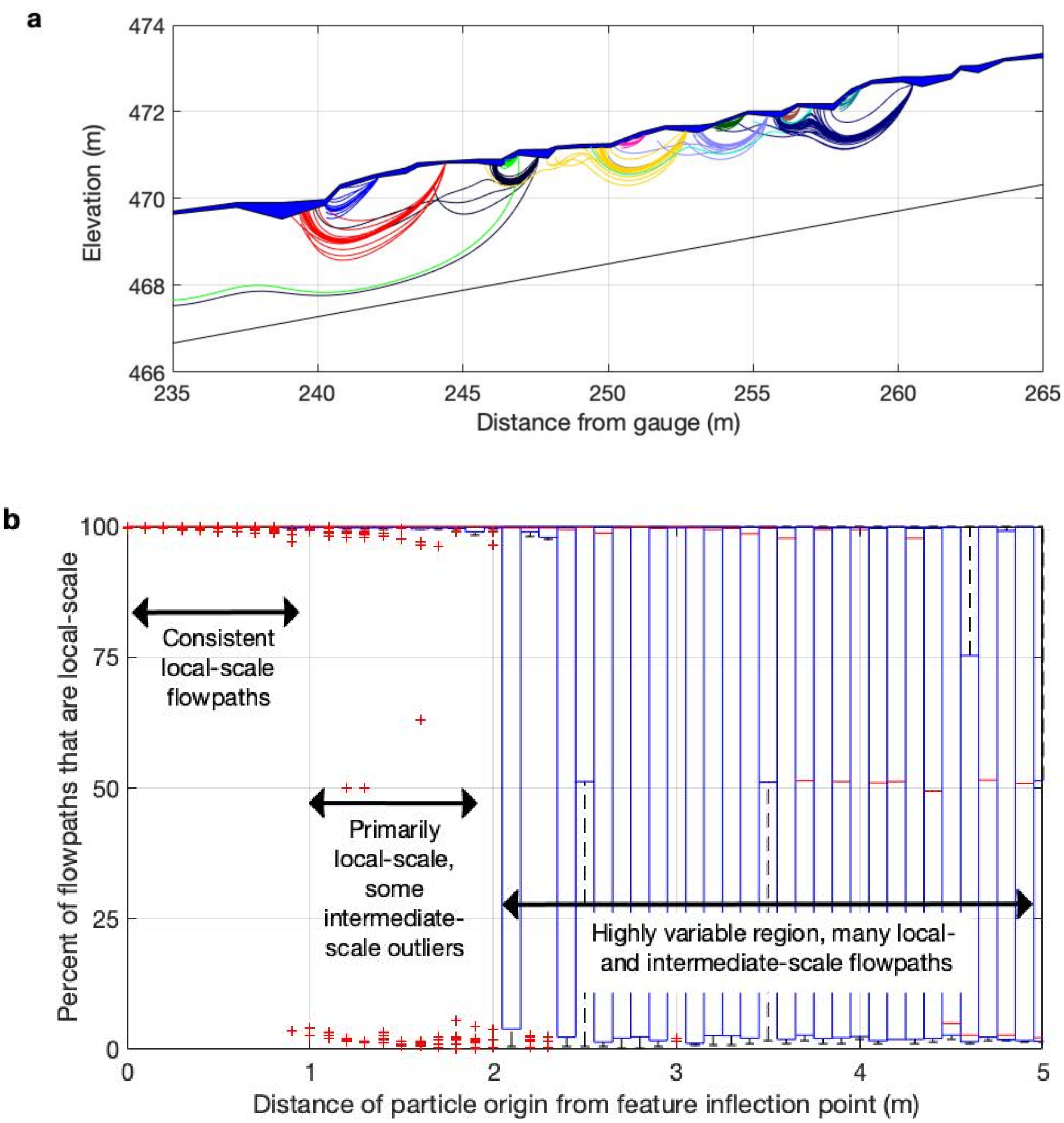

Figure 1. Cumulative particle traces for all simulations (n=361) for one central particle and one distal particle each from Features 33-38 (i.e., a zoomed in view of representative features near the center of the model domain), plotted onto basecase topography (a). Each particle has a different color, but the colors are held constant for all simulations. Flowpaths that do not fully return to the streambed are due to differences between the basecase topography and the modified topography of a given simulation. Box and whisker plots (b) show the percentage of hyporheic flowpaths that are local-scale (i.e., not intermediate-scale) as a function of particle origin location relative to the central inflection point of each feature (n=60). The red bar on each box plot represents the median, the box spans the 25th to 75th percentiles, the whiskers span the 9th to 91st percentiles, and red crosshairs are outliers. Only particles upstream from the inflection point are shown, because downstream particles upwelled immediately at basecase.

3.2 A small number of streambed locations are both sensitive and influential

We evaluated which flowpaths were sensitive to manipulations of each focal feature in the scenarios in which feature heights were changed by ±50% (Figure 2). According to the common assumption that features behave independently (explicit in upscaling studies and implicit in analyses of isolated features), one would expect that -50% scenarios would cause decreased flowpath lengths within the focal feature and +50% would increase flowpath lengths (as in Hester & Doyle, 2008), and neighboring features would be unaffected. In all scenarios the significant flowpath changes tended to be centered on the focal feature (visible as the diagonal band of dark color in Figure 2 and Figure S5), but also associated with neighboring features (i.e., outside of the black dots marking the boundaries of each focal feature). For example, a -50% manipulation of features 6 and 38 reduced flowpath lengths in the focal features and caused subtle increases in flowpath lengths within neighboring features. In some cases a -50% manipulation caused some flowpaths within the focal feature to lengthen and others to get smaller (e.g., Features 15 and 61), but decreasing feature height never caused all flowpaths within the focal feature particles to increase. Patterns for -10% and -25% were similar but less pronounced than for -50% (Figure S5).

Changes in the +50% scenario were generally in the same location but opposite direction compared to the -50% results (Figure 2). That is, +50% manipulations tended to lengthen flowpaths within a focal feature and decrease flowpath lengths in neighboring features. Overall these patterns were comparable but more subtle in the +10% and +25% scenarios (Figure S5). However, +50% produced greater and more extended feature influences than -50% scenario (mean feature influence and mean flowpath sensitivity panels in Figure 2). Positive stretching scenarios sometimes caused water to pond immediately upstream of the focal feature, producing a more distributed but variable impact on the model domain. For example, several features (e.g., 9, 27, 44, 52) unexpectedly produced only decreases in flowpath lengths within the focal feature during +50% scenarios. In many cases for both the +50% and -50% scenarios, flowpaths originating at neighboring features were as sensitive or more sensitive than those originating at the focal feature (e.g, focal features 23, 31, 43, and 53). Thus, our systematic manipulations showed that feature-feature interactions can be important in modifying hyporheic flowpath geometry.

Not all features were equally influential, and not all flowpaths were equally sensitive to changes. The two features that were shortest in length (i.e., 37 and 41) generated no significant changes in any flowpaths for both ±50%. In contrast, a small number of features were so influential that the average change across all particles was >5% (Figure 2 top panels). The exact features exceeding the 5% average flowpath change were variable based on the manipulations, and positive manipulations generally had a greater effect than the negative manipulations, likely due to their previously discussed impacts on the local hydraulic head profile. Nevertheless, features 15, 27, 31, 40, 43, 53, and 55 (centered at X = 150, 210, 230, 265, 280, 320, and 335 meters along the reach) were the most consistent, meeting this 5% average flowpath change threshold in at least 3/6 scenarios. These features tended to be taller and longer than the average feature, but these characteristics were not sufficient to explain their influence, as 4 other features ranked in the top 10 of both height and length but did not generate the same level of influence. For flowpath sensitivity, the most consistently variable (i.e., >50% average sensitivity in 3/6 scenarios) regions were apparent as horizontal bands in the main and right panels (e.g., flowpaths 650, 700, 1200, 1800, 1950, and 2400; Fig. 2), which corresponded to Features 15, 16, 28, 41, 44, and 54. Spatially, these bands were more commonly generated to the left of the focal feature

1:1 line than to the right, meaning that particles are more sensitive to downstream changes in topography than to upstream changes. With the exception of feature 15, which was also one of the most influential features, features with particularly sensitive particles tended to be shorter in height but not shorter in length than average. Instead, the common characteristic of the sensitive features is that they were located next to influential features, revealing a set of paired locations that are both sensitive and influential.

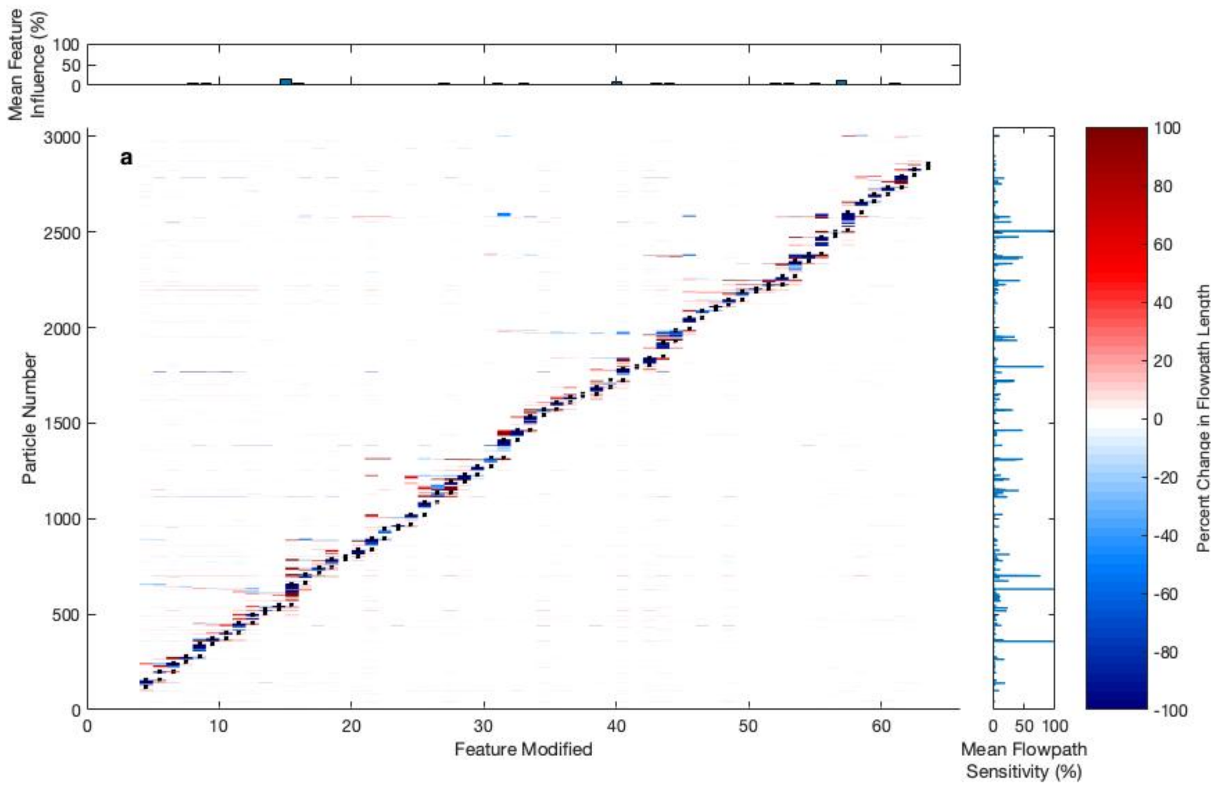

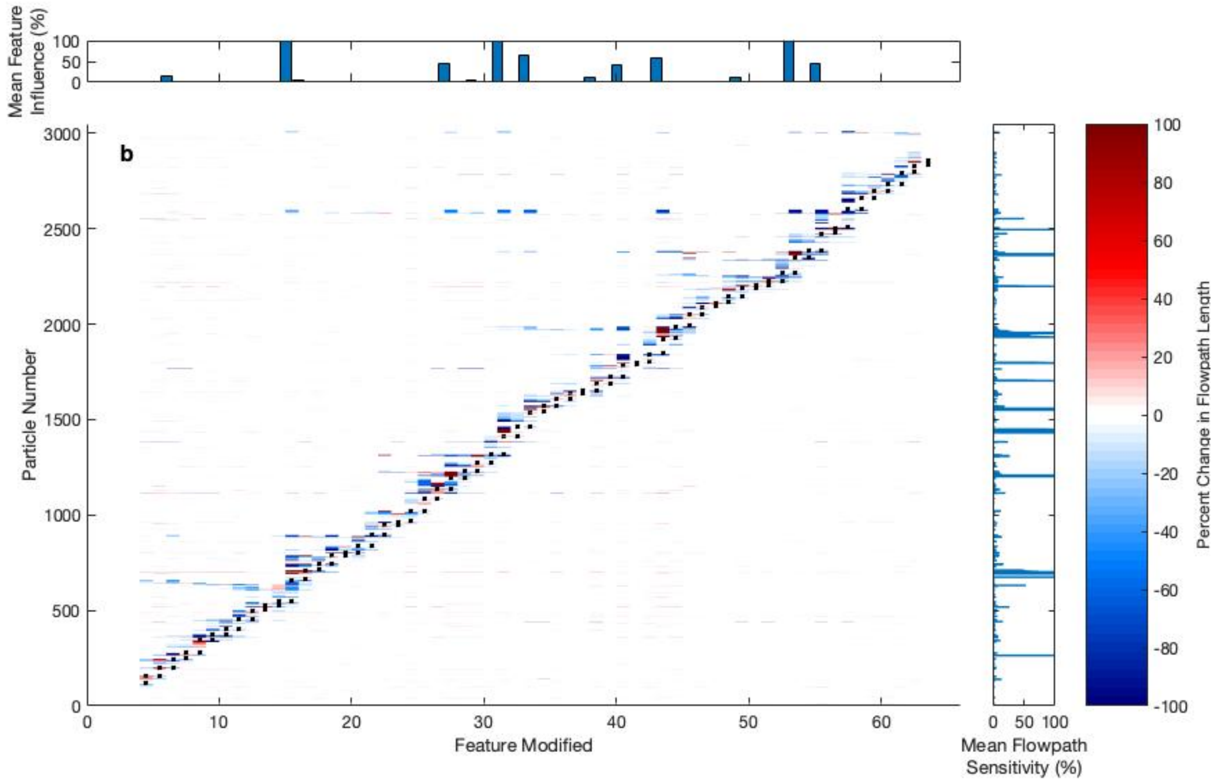

Figure 2. Normalized % change in flowpath length for each feature stretched -50% (a) and +50% (b). Black dots mark the range of particles associated with each focal feature. Panels above and to the right of each plot show the average of columns and rows, representing the mean feature impact and mean flowpath variability, respectively.

<u>3.3 Certain locations act as hyporheic turnover points</u>

Some flowpaths never exceeded a few meters in length across all simulations, while others varied over orders of magnitude (Fig. 3). Locations where we observed significant variation in flowpath lengths were consistently downwelling in nearly all simulations (vertical "columns" of particles in Fig. 3). The points in a column reflect the travel distances for particles released from any given location, a spatial equivalent to a forward transit time distribution (distribution of timescales for all particles starting at a given time). Columns with large variation in flowpath lengths indicate downwelling locations that were highly sensitive to channel morphology. Gaps visible within the columns reflect the prior observation that intermediate flowpaths cannot upwell just anywhere, but are instead restricted to upwelling at the distal regions at the edges of local hyporheic flow cells. In addition to the analogue for forward transit time distributions, we also note a parallel interpretation to a backward transit time distribution. Diagonal lines show particles that enter the hyporheic zone at many different points upstream, but all upwell at the same location (where the diagonal intersects y=0). Thus, these diagonals can be interpreted as a backward transit distribution, with particles having traveled a range of distances depending on manipulations but sharing an upwelling location. The diagonals are slightly steeper than a 1:1 line because flowpath length includes a small vertical component in addition to distance along the x-axis. These diagonal lines terminate immediately upstream from the columns, showing that consistent downwelling at the column also truncates flowpaths originating at a wide range of upstream points in the reach.

The co-location of "columns" and "diagonals" in Figure 3, representing upwelling and downwelling of intermediate-scale flowpaths, respectively, demonstrates that intermediate-scale hyporheic exchange was limited to a small number of specific locations in the reach. Strong downwelling at the columns forces a large proportion of the subsurface downvalley flow to upwell back to the stream. Put another way, turnover of deep hyporheic water was concentrated at a few locations where downvalley flows originating higher in the reach were truncated, and new intermediate-scale hyporheic flowpaths originated. This interpretation explains why a small number of locations (hereafter called "turnover points", which are explored further below) can impact distant upstream flowpaths. In turn, new downwelling flowpaths may be truncated by additional, downstream turnover points in our vertically constrained domain.

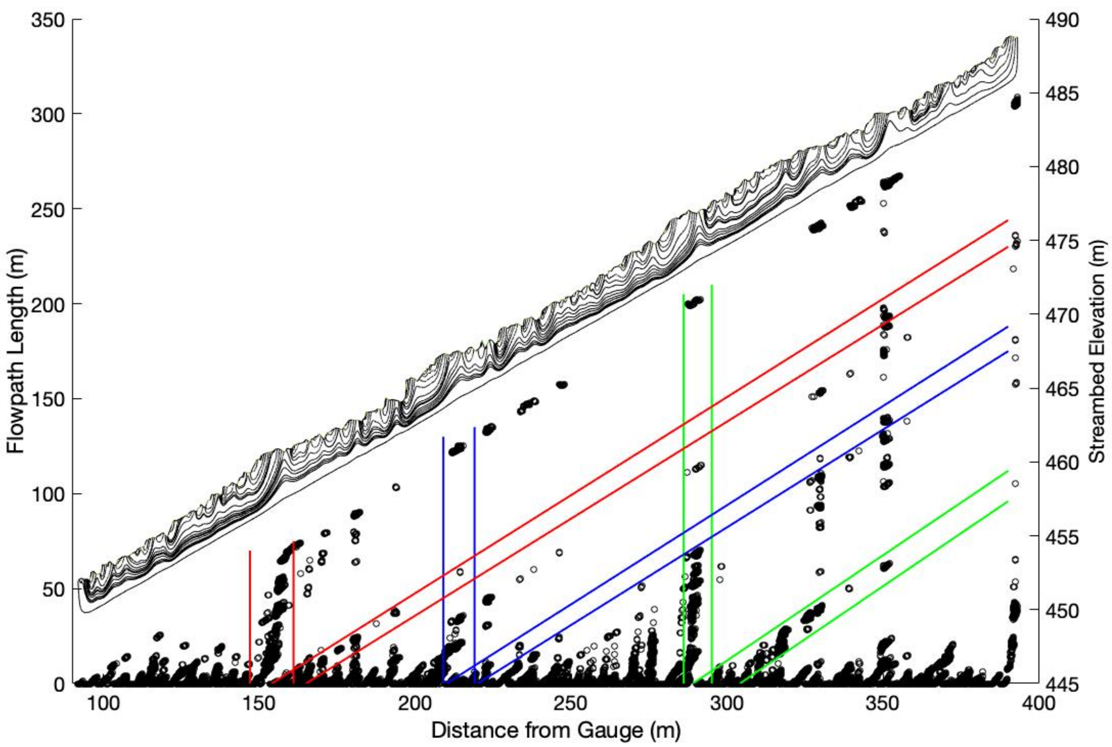

Figure 3. Scatter of flowpath lengths for each particle across 361 manipulations (each point is one flowpath from one simulation; left y-axis). The highlighted columns and diagonals visualize the travel distances for particles released from any given location (columns) and the particles released from many different locations that upwell at the same point (diagonals). The intersection of columns and diagonals mark key locations of hyporheic turnover. The basecase streambed and flowpath geometries are shown for context (right y-axis).

3.4 Intermediate-scale topography dictates turnover points

The power spectral density revealed a series of dominant wavelengths, with a natural break between the four most important (ranging from 50-300 m), and a secondary group between 10-50 m (Figure S6). Notably, the local feature-scale (i.e., <10 m) was indistinguishable from random noise. The MATLAB Curve Fitting Tool, also based on Fourier transforms, generated sine waves that were well aligned with the periodogram (Table S1). Using the curve fitting tool, objective functions (R^2, SSE, RMSE) only improved marginally after considering more than four wavelengths (Figure S7). Thus we proceeded by approximating the topography as the sum of 4 sine waves ($R^2 = 0.75$), which provided a parsimonious model and reasonably matched the smoothed, larger-scale topography (Figure 4a).

The sum-of-sines topography shows 3 intermediate-scale features in the center of the model domain. Although slightly irregular, these intermediate features are each expected to generate downwelling and upwelling in the same way as the local-scale features that are superimposed on them. The amplitude of these intermediate features was approximately 1 m, which was comparable to the heights of local-scale features (mean 0.7 m, st. dev. 0.4 m). Despite their similar heights, the intermediate features had wavelengths on the order of 100 m, compared to local-scale features that were 4.5 ± 2.1 m long (mean ± st. dev.). The extended length of the intermediate features made them difficult to see, both in the model and in the field. It is not clear what caused their formation (e.g., debris-flow deposits with log jams or landslide deposits from adjacent hillslopes that were not mobilized into debris flows, or perhaps some underlying geologic structure that fixes these locations in space). Regardless of their origin, the intermediate-scale features exerted a strong influence on subsurface hydrology; the turnover points clearly align with intermediate-scale downwelling locations (Fig. 4b). Although the co-location is visually apparent, the intermediate features alone do not explain why some turnover points are clustered into wider bands (e.g., those at X = 160, 215, 290, 350), or why a few turnover points are located on the upwelling side of the intermediate-scale features (i.e., those at X = 120, 190). To fully understand what controls the location of turnover points, the local- and intermediate-scales must be superimposed together. The widest bands of the downwelling locations result from alignment of large local features and intermediate peaks, with the two scales of downwelling reinforcing each other to generate extra steep gradients. Likewise, the turnover points found in intermediate upwelling zones were due to large local features that were strong enough to overwhelm upwelling caused by the intermediate-scale features. Thus, local- and intermediate-scale features interact to determine key locations of hyporheic exchange and may reinforce or oppose each other depending on their topology.

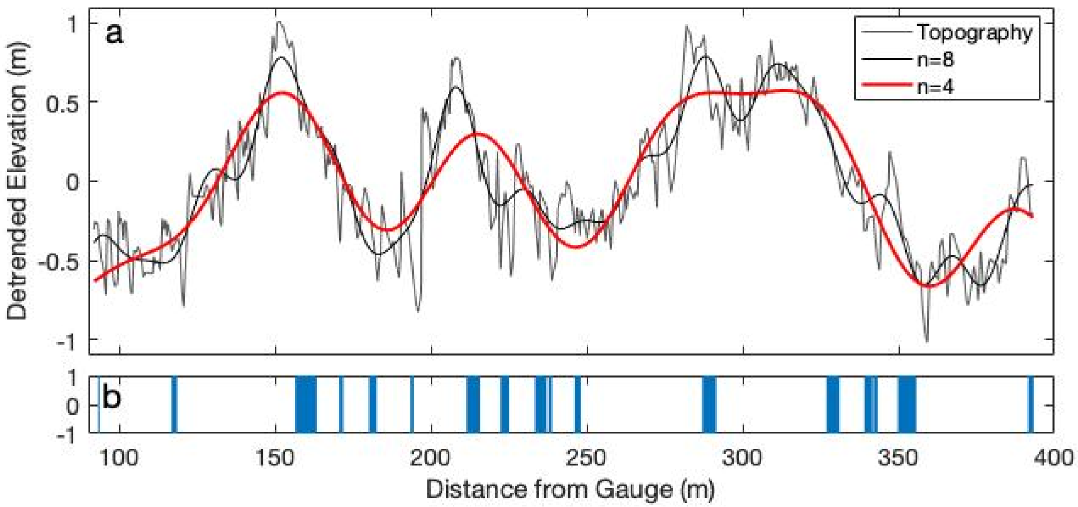

Figure 4. (a) Detrended topography and model fits for n = 4 and n = 8 sine waves, and (b) locations of turnover points (locations of columns in Figure 3). The width of blue bars is proportional to the length of intermediate downwelling zones.

4. Discussion

4.1 At the reach-scale, how sensitive are flowpaths to manipulations of individual features?

Flowpath sensitivity to morphology was not uniform along our study reach. At the local-scale, particles that downwelled near the center of features were tightly held by steep head gradients and thus unlikely to switch scales during the simulations. However, flowpaths that downwelled near the upstream end of a feature were more weakly associated with that feature and more sensitive to changes – reminiscent of loosely held high orbital electrons in an atom. These more distal local flowpaths were more often changed into intermediate flowpaths (switching from a single-feature association to spanning multiple features), or compressed to make room for intermediate upwelling. Schmadel et al. (2017) found similar trends (using the same basecase geometry model): across 9 different discharge and groundwater upwelling scenarios, flowpaths <1 m long were consistently more stable than flowpaths of 1-10 m. At the larger-scale, we found that individual intermediate flowpaths were also sensitive, but the overall regions of intermediate upwelling and downwelling only shifted slightly across 360 simulations (Figure 3). In other words, effective intermediate-scale geometry was minimally impacted by common local-scale changes. Instead, we found that intermediate-scale flowpath geometry was primarily controlled by the superposition of intermediate-scale topography and individual large, local features. That is, local-scale features and intermediate-scale features could reinforce each other where the crests and troughs were aligned. Conversely, the different scales could oppose each other where they were out of alignment. Several large local-scale features were even able to drive intermediate-scale downwelling in places where the intermediate-scale topography would otherwise have generated upwelling.

4.2 Strange (stream)bedfellows: feature-feature interactions can play an important role in headwater stream reaches

State of the science models for upscaling feature- and reach-scale results to the network- or continental-scales rely on the assumption that, regardless of their scale, features operate independently and can be accumulated additively (Gomez-Velez & Harvey, 2014). This assumption also applies implicitly to individual features, as the influences of neighboring features of the same scale are not considered by most studies (Schmadel et al., 2017). Neglecting feature-feature interactions may be valid in low gradient dune-ripple systems where hydrostatic head gradients are weak. However, our results show that step-pool sequences can have significant impacts on their neighbors in high gradient mountain streams. In our study, the majority of features, when modified, produced significant alterations of some flowpaths in neighboring features – typically the immediate neighbors, but occasionally even distant features. This phenomenon is specific to the morphology of the feature modified, morphology of neighboring features, and feature topology. As a consequence, our findings are not readily generalizable, but are in agreement with past studies of mountain headwaters. Gooseff et al. (2006) found that a pool-step-riffle produced 60% downwelling and 40% upwelling, whereas a rearranged but otherwise identical riffle-step-pool reversed these percentages. In another study, the amount of hyporheic exchange flux associated with one large step was greater than 10 small steps of the same total height (Kasahara & Wondzell, 2003), presumably due to feature-feature interference. This earlier work suggested that both the order of features as well as their individual sizes was important in determining the hyporheic flowpath lengths and timescales in a given reach.

4.3 What is the role of shallow bedrock in multi-scale interactions?

The local and intermediate step-pool features in WS01 had comparable heights and amplitudes, resulting in multi-scale interaction. As a result, these scales would not be easily deconvolved as in Stonedahl et al. (2013) and the NEXSS model (Gomez-Velez & Harvey, 2014). In fact, whenever the transport timescales associated with different exchange processes overlap, it becomes difficult to isolate the effects of any single exchange scale (e.g., Wlostowski et al., 2017). Payn et al. (2009) argued that the key to understanding reach-scale flows and transit times is predicting where intermediate flowpaths initiate and terminate. Our study reinforces this point because intermediate-scale exchange often occurred at locations where local and intermediate peaks aligned. Thus, simple analysis of the surface topography – which can be quickly parameterized from ground-based or aerial surveys – may reveal the key locations of intermediate-scale hyporheic turnover. In between such locations, the hyporheic zone may be conceptualized as a spatially binary system: shallow hyporheic flow cells associated with local-scale features operate relatively independently from deeper downvalley flows (Figure 5). Many studies have shown that the relatively steep hydraulic gradients across local-scale features reduce the importance of intermediate- and regional-scale flowpaths, such that local-scale, shallow hyporheic flow cells account for the majority of hyporheic exchange flux in a reach (Chow et al., 2018; Morén et al., 2017; Stonedahl et al., 2010; C. Wang et al., 2018). However, the turnover points were important in causing nearly complete exchange of hyporheic porewater, acting as a switch for the binary tracks. In our 2-D model, this pattern is caused by preferential filling of downvalley flow capacity by steep local-intermediate feature alignments, forcing upstream hyporheic water to upwell. It is likely that comparable patterns exist in 3-D, as Kasahara and Wondzell (2003) showed substantial interactions among a wide range of feature types that cannot be simulated in our 2-D vertical-profile model domain.

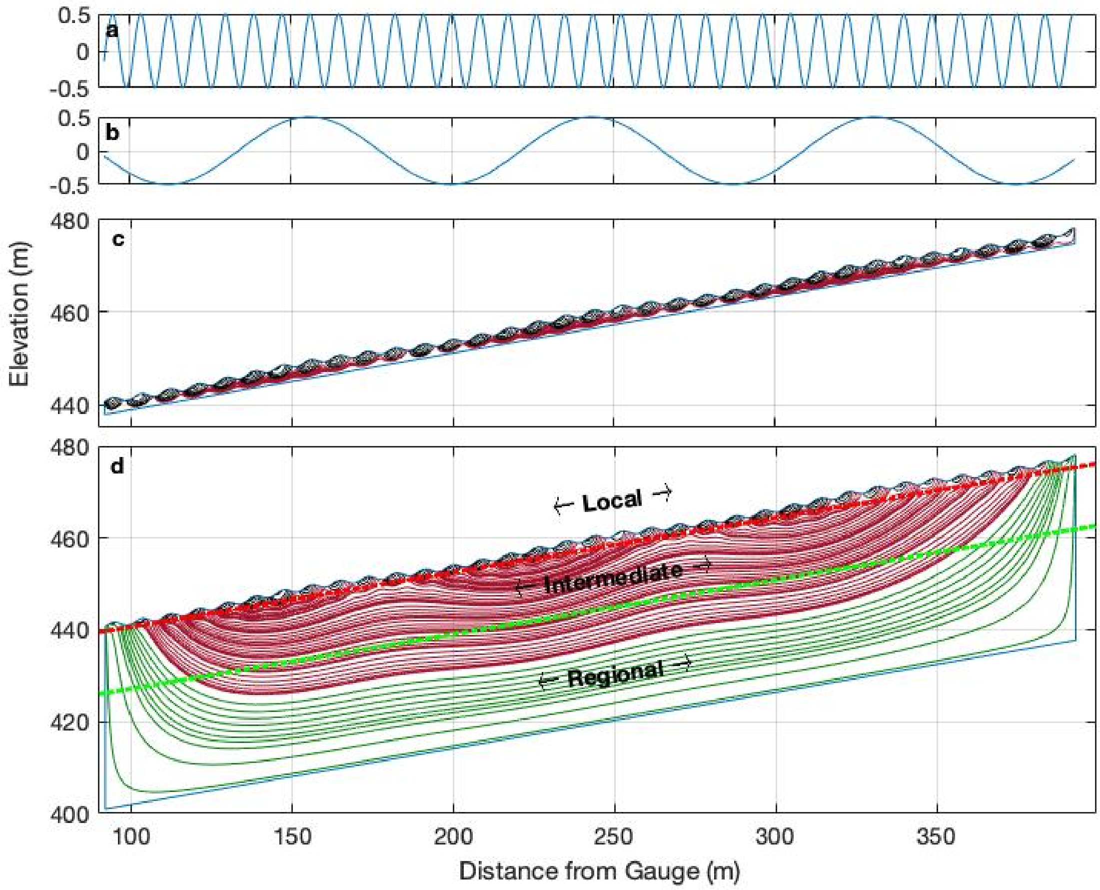

Figure 5. (a) Idealized local topography (amplitude = 1 m, wavelength = 4.5 m); (b) idealized intermediate topography (amplitude = 1 m, wavelength = 45 m); (c) resultant (local + intermediate) topography in shallow (3 m) hyporheic zone with intermediate flowpaths highlighted in red; and (d) resultant (local + intermediate) topography and flowpaths in deep (40 m) hyporheic zone with intermediate flowpaths highlighted in red and regional in green. For reference, the theoretical divides between local-intermediate and intermediate-regional flows are also plotted at the depth equal to one third of the local and intermediate wavelengths, respectively.

Why do the intermediate features cause such complete hyporheic turnover? Any given location within the streambed is affected by a range of topographic scales, both near and distant, with larger wavelengths influencing proportionally greater depths (Tóth, 1963; Wörman et al., 2007). However, bedrock can shield shallower flowpaths from distant and low frequency features (Cardenas & Jiang, 2010; Mojarrad et al., 2019; Wörman et al., 2007). Mojarrad et al. (2019) showed that net hyporheic exchange decreased with greater hyporheic zone depth in a multi-scale system, likely due to increased interference from larger-scales as bedrock shielding decreased. In particular, bedrock exerts increasing influence as wavelengths approach and exceed 3 times the sediment depth (Wörman et al., 2007). Our model assumed a uniform 3 m depth to bedrock based on previous work in the H.J. Andrews (Gooseff et al., 2006; Schmadel et al., 2017). Accordingly, the local-scale step features with wavelengths <9 m did not interact with the bedrock, allowing for the binary local-downvalley system to prevail. However, the intermediate-scale features had wavelengths an order of magnitude greater than the ~9 m threshold, so they were able to drive flow far deeper into the HZ, nearly to the no-flow boundary. These turnover points cutoff downvalley transport and produced intermediate-scale flows in our model, but a system with deeper sediments and/or shorter wavelengths (i.e., wavelengths <3 times the depth) would develop regional flows from the global maximum to the global minimum elevations.

The ability of intermediate downwelling to truncate upstream flowpaths means that downstream features exert a control on the fate of hyporheic water that originated in upstream features. Because of the relatively long intermediate-scale feature wavelength, there are multiple local feature downwelling zones aligned with the intermediate-scale downwelling zones. However, intermediate downwelling is most pronounced at the peak of an intermediate feature, because that is the downstream-most location of alignment between local- and intermediate-scales. The reasons for this are two-fold: the intermediate-scale contribution to downwelling, and thus the total vertical hydraulic gradient, is strongest in the center of the feature (more central flowpaths being tightly held), and the last local feature can also block its upstream neighbors.

4.4 Challenges and opportunities for upscaling in high-gradient stream networks

The lengths of intermediate-scale flowpaths are independent from the features that initiated them. Rather, the intermediate flowpaths penetrate deep into the hyporheic zone, where they travel downvalley until they are forced upward by one of several processes. In our 2-D model this forcing occurs in two ways: 1) where the hyporheic sediment thickness is abruptly reduced, or 2) wherever downwelling is sufficiently strong to overwhelm these downvalley flows. The former occurred below tall steps and at the end of the model domain, whereas the latter occurred where the next downstream intermediate-scale feature aligned with a local-scale feature. Because local-scale features were common enough to come close to aligning with the crests of intermediate-scale features, just by chance, the actual locations of the turnover points was determined by the location of the intermediate-scale feature. Thus, the spacing of these intermediate-scale features determined the approximate intermediate flowpath geometries for the entire reach we studied. Individual feature manipulations, representative of episodic deposition and degradation of logs and debris, did not affect the general location of intermediate flowpaths, instead they revealed the persistence of turnover points.

In a prior study of the same reach, stream discharge was not found to be a primary control on hyporheic flow in WS01, with the exception of very low flows in which the stream became intermittent (Schmadel et al., 2017). Together with our results, these observations show that changes in local topography and discharge are not primary controls on intermediate hyporheic cell geometries. This highlights the role of geologic setting, in which the hyporheic zone flow capacity is determined by sediment depth, hydraulic conductivity, and valley slope rather than surface water levels, and the multi-scale topography further controls hyporheic exchange via turnover points. Notably, we did not consider the role of hydraulic conductivity heterogeneities and anisotropy from poorly sorted colluvium or streambed armoring, nor the potential influence of non-planar bedrock topography. The impacts of these variables are hard to predict, as they could enhance or reduce multi-scale interactions depending on site-specific realizations. For example, if boulders and other relatively impermeable heterogeneities spanned the majority of the hyporheic depth (and cross-section) they could isolate hyporheic flow cells, whereas smaller and shallower obstacles could force hyporheic cells to travel deeper and further through the HZ before upwelling (Vaux, 1968; Ward et al., 2012). Likewise, vertical anisotropy is expected to reduce the effective hyporheic zone depth relative to regional downvalley flows, but any local-scale features that overcame the anisotropy would be more likely to generate longer intermediate-scale flowpaths. Other studies have found additional aspects of geologic setting that truncate downvalley flows, such as focused groundwater inflows from lateral tributary valleys (Schmadel et al., 2017) and reductions in the hyporheic zone depth (1-D) or cross-section (2-D) (Tonina & Buffington, 2009; Vaux, 1968; Ward et al., 2012). Hydrodynamic head, discharge variation, and the interaction between streambed topography and stream depth were neglected in our study because they are expected to be far smaller than static head gradients across step-pools (after Schmadel et al., 2017; Ward et al., 2018b). However, all three processes are increasingly relevant at lower gradients where they could further enhance or reduce the local hydraulic gradients resulting from multi-scale interactions of topographic features. Future work should investigate the role of gradient and corresponding changes in stream morphology, discharge, and stream size that may control the relevance of multi-scale interactions.

A 1-D network-scale hyporheic zone model like Ward et al. (2018a), which already considers the hyporheic cross-sectional area as a truncation mechanism, could be readily updated to also include hyporheic exchange from intermediate turnover points (detected by spectral analysis of LiDAR or survey data). Notably, this would increase the estimates of total hyporheic exchange in steep mountain catchments beyond that predicted from fluctuations in HZ capacity alone, due to preferential filling of capacity with fresh streamwater at intermediate features. Further, the truncation of downvalley flowpaths into intermediate hyporheic cells would shift the binomial residence time distributions (local and regional found in Ward et al., 2018a) toward a more continuous distribution with fewer late-time flowpaths. Future work should evaluate the presence of overlapping scales in other mountain catchments, and incorporate them into upscaling efforts for water resources management. For example, our results could inform efforts such as that by Magliozzi et al. (2018) to identify priority areas for stream restoration. In particular, multi-scale designs could emphasize or reduce intermediate flowpaths depending on the residence times associated with biogeochemical processes of interest.

5. Conclusions

Multi-scale models are essential to predict hyporheic fluxes and transit times across unstudied reaches and entire stream networks. This information has many practical uses for river management, from delineating connectivity within river corridors to identifying priority areas for stream restoration. In lowland rivers, the independence of spatial and temporal scales of exchange allows relatively simple, additive upscaling. In this study we examined whether the same technique would be possible for steep mountain catchments. Notably, we only considered hydrostatic forces in this analysis as they are expected to be dominant. Unlike lowland rivers, we found that hyporheic flowpaths were strongly dependent on both local and intermediate context: many local-scale features influenced neighboring features and had further interactions with a larger, intermediate-scale of topography.

Despite the observed complexity and sensitivity of hyporheic flowpaths, simplified upscaling may still be possible based on the interaction of topographic wavelengths with streambed depth. In shallow HZ, intermediate flowpaths can cause nearly complete turnover of hyporheic porewater, truncating downvalley flows and shielding features from distant topography. We build on a three-track conceptual model in which local, intermediate, and regional flowpaths can be approximated from likely start and endpoints according to the streambed topography and bed depth. In shallow systems like WS01 and/or systems with long topographic wavelengths, the regional-scale may disappear entirely.

Finally, local feature-feature interactions should be explicitly considered during field monitoring studies and restoration of streams and floodplains. The spacing of individual features (e.g., cross-vanes, large woody debris) matters: two features too close together may primarily generate intermediate flowpaths rather than doubling the exchange of either individual feature in isolation. Either case may be desirable depending on site specific characteristics and processes of interest. Put another way, when monitoring hyporheic water quality, the flowpath you are measuring may not belong to the local feature you are standing at. In our system for example, upwelling water at a prominent feature (Feature 25 at X = 195-200) is more likely to have originated 10m upstream in Features 26 and 27 than from Feature 25 itself. As Buffin-Bélanger and Roy (2000) describe for surface turbulent flows, the complex interactions between multi-scale features are as important as the individual features themselves. Field monitoring and restoration designs should attend to the placement of multi-scale features (e.g., log jams, wetlands, paleochannels, and meanders) in the same way that wind farm optimization considers the siting of individual windmills (local-scale) and windmill clusters (intermediate-scale) within the larger-scale valley setting (regional-scale) to maximize power production (Kusiak & Song, 2010). Predictability of multi-scale hyporheic interactions in mountain watersheds is critical to protecting and restoring valuable ecosystem services.

Acknowledgments, Samples, and Data

Data and facilities were provided by the HJ Andrews Experimental Forest and Long Term Ecological Research program, administered cooperatively by the USDA Forest Service Pacific Northwest Research Station, Oregon State University, and the Willamette National Forest and funded, in part, by the National Science Foundation under Grant No. DEB-1440409. Additional support was provided by National Science Foundation awards EAR 1652293, EAR 1417603, and EAR 1446328 and Department of Energy award DE-SC0019377. Additional support was provided by the home institutions of the authors. Any use of trade, firm, or product names is for descriptive purposes only and does not imply endorsement by the US Government. Any opinions, findings, and conclusions or recommendations expressed in this material are those of the authors.

All authors contributed to the conceptual design of the study and manuscript preparation. The basecase model was developed by NMS. SPH led additional simulations, data analysis, and manuscript preparation. The authors report no conflicts of interest.

Model input data (streambed topography, water surface) and metrics for particle tracks (release location, upwelling location, flowpath length and timescale, velocity at release location) are available at: <<Authors to insert doi from CUAHSI HydroShare here after manuscript is accepted, as the doi cannot be assigned without all metadata, and metadata cannot be completed without knowing the doi of the published paper>>.

References

Alexander, L. C., Fritz, K. M., Schofield, K. A., Autrey, B. C., DeMeester, J. E., Golden, H. E., et al. (2018). Featured Collection Introduction: Connectivity of Streams and Wetlands to Downstream Waters. *JAWRA Journal of the American Water Resources Association*, *54*(2), 287–297. https://doi.org/10.1111/1752-1688.12630

Alexander, R. B., Boyer, E. W., Smith, R. A., Schwarz, G. E., & Moore, R. B. (2007). The Role of Headwater Streams in Downstream Water Quality1. *JAWRA Journal of the American Water Resources Association*, *43*(1), 41–59. https://doi.org/10.1111/j.1752-1688.2007.00005.x

Aubeneau, A. F., Hanrahan, B., Bolster, D., & Tank, J. (2016). Biofilm growth in gravel bed streams controls solute residence time distributions. *Journal of Geophysical Research: Biogeosciences*, *121*(7), 1840–1850. https://doi.org/10.1002/2016JG003333

Bao, J., Zhou, T., Huang, M., Hou, Z., Perkins, W., Harding, S., et al. (2018). Modulating factors of hydrologic exchanges in a large-scale river reach: Insights from three-dimensional computational fluid dynamics simulations. *Hydrological Processes*, *32*(23), 3446–3463. https://doi.org/10.1002/hyp.13266

Boano, F., Revelli, R., & Ridolfi, L. (2007). Bedform-induced hyporheic exchange with unsteady flows. *Advances in Water Resources*, *30*(1), 148–156. https://doi.org/10.1016/J.ADVWATRES.2006.03.004

Boano, F., Revelli, R., & Ridolfi, L. (2008). Reduction of the hyporheic zone volume due to the stream-aquifer interaction. *Geophysical Research Letters*, *35*(9), L09401. https://doi.org/10.1029/2008GL033554

Boano, F., Harvey, J. W., Marion, A., Packman, A. I., Revelli, R., Ridolfi, L., & Wörman, A. (2014). Hyporheic flow and transport processes: Mechanisms, models, and biogeochemical implications. *Reviews of Geophysics*, *52*(4), 603–679. https://doi.org/10.1002/2012RG000417

Boulton, A. J., Findlay, S., Marmonier, P., Stanley, E. H., & Valett, H. M. (1998). THE FUNCTIONAL SIGNIFICANCE OF THE HYPORHEIC ZONE IN STREAMS AND RIVERS. *Annual Review of Ecology and Systematics*, *29*(1), 59–81. https://doi.org/10.1146/annurev.ecolsys.29.1.59

Brunke, M., & Gonser, T. (1997). The ecological significance of exchange processes between rivers and groundwater. *Freshwater Biology*, *37*(1), 1–33. https://doi.org/10.1046/j.1365-2427.1997.00143.x

Buffin-Bélanger, T., & Roy, A. G. (2000). Vers l'intégration des structures turbulentes de l'écoulement dans la dynamique d'un cours d'eau à lit de graviers. *Géographie Physique et Quaternaire*, *54*(1), 105. https://doi.org/10.7202/004776ar

Cardenas, M. B. (2015). Hyporheic zone hydrologic science: A historical account of its emergence and a prospectus. *Water Resources Research*, *51*(5), 3601–3616. https://doi.org/10.1002/2015WR017028

Cardenas, M. B., & Jiang, X.-W. (2010). Groundwater flow, transport, and residence times through topography-driven basins with exponentially decreasing permeability and porosity. *Water Resources Research*, *46*(11). https://doi.org/10.1029/2010WR009370

Cardenas, M. B., & Wilson, J. L. (2007). Exchange across a sediment–water interface with ambient groundwater discharge. *Journal of Hydrology*, *346*(3–4), 69–80. https://doi.org/10.1016/J.JHYDROL.2007.08.019

Caruso, A., Boano, F., Ridolfi, L., Chopp, D. L., & Packman, A. (2017). Biofilm-induced bioclogging produces sharp interfaces in hyporheic flow, redox conditions, and microbial community structure. *Geophysical Research Letters*, *44*(10), 4917–4925. https://doi.org/10.1002/2017GL073651

Castro, N. M., & Hornberger, G. M. (1991). Surface-subsurface water interactions in an alluviated mountain stream channel. *Water Resources Research*, *27*(7), 1613–1621. https://doi.org/10.1029/91WR00764

Chow, R., Wu, H., Bennett, J. P., Dugge, J., Wöhling, T., & Nowak, W. (2018). Sensitivity of Simulated Hyporheic Exchange to River Bathymetry: The Steinlach River Test Site. *Groundwater*. https://doi.org/10.1111/gwat.12816

Day-Lewis, F. D., Linde, N., Haggerty, R., Singha, K., & Briggs, M. A. (2017). Pore network modeling of the electrical signature of solute transport in dual-domain media. *Geophysical Research Letters*, *44*(10), 4908–4916. https://doi.org/10.1002/2017GL073326

Dehkordy, F. M., Briggs, M. A., Day-Lewis, F. D., Singha, K., Krajnovich, A., Hampton, T. B., et al. (2019). Multi-scale preferential flow processes in an urban streambed under variable hydraulic conditions. *Journal of Hydrology*. https://doi.org/10.1016/J.JHYDROL.2019.03.022

Fox, A., Boano, F., & Arnon, S. (2014). Impact of losing and gaining streamflow conditions on hyporheic exchange fluxes induced by dune-shaped bed forms. *Water Resources Research*, *50*(3), 1895–1907. https://doi.org/10.1002/2013WR014668

Gomez-Velez, J. D., & Harvey, J. W. (2014). A hydrogeomorphic river network model predicts where and why hyporheic exchange is important in large basins. *Geophysical Research Letters*, *41*(18), 6403–6412. https://doi.org/10.1002/2014GL061099

Gomez-Velez, J. D., Harvey, J. W., Cardenas, M. B., & Kiel, B. (2015). Denitrification in the Mississippi River network controlled by flow through river bedforms. *Nature Geoscience*, *8*(12), 941–945. https://doi.org/10.1038/ngeo2567

Gooseff, M. N., Wondzell, S. M., Haggerty, R., & Anderson, J. (2003). Comparing transient storage modeling and residence time distribution (RTD) analysis in geomorphically varied reaches in the Lookout Creek basin, Oregon, USA. *Advances in Water Resources*, *26*(9), 925–937. https://doi.org/10.1016/S0309-1708(03)00105-2

Gooseff, M. N., Anderson, J. K., Wondzell, S. M., LaNier, J., & Haggerty, R. (2006). A modelling study of hyporheic exchange pattern and the sequence, size, and spacing of stream bedforms in mountain stream networks, Oregon, USA. *Hydrological Processes*, *20*(11), 2443–2457. https://doi.org/10.1002/hyp.6349

Grant, S. B., Gomez-Velez, J. D., & Ghisalberti, M. (2018). Modeling the Effects of Turbulence on Hyporheic Exchange and Local-to-Global Nutrient Processing in Streams. *Water Resources Research*, *54*(9), 5883–5889. https://doi.org/10.1029/2018WR023078

Hester, E. T., & Doyle, M. W. (2008). In-stream geomorphic structures as drivers of hyporheic exchange. *Water Resources Research*, *44*(3). https://doi.org/10.1029/2006WR005810

Kasahara, T., & Wondzell, S. M. (2003). Geomorphic controls on hyporheic exchange flow in mountain streams. *Water Resources Research*, *39*(1), SBH 3-1-SBH 3-14. https://doi.org/10.1029/2002WR001386

Kennedy, V. C., Jackman, A. P., Zand, S. M., Zellweger, G. W., & Avanzino, R. J. (1984). Transport and concentration controls for chloride, strontium, potassium and lead in Uvas Creek, a small cobble-bed stream in Santa Clara County, California, U.S.A.: 1. Conceptual model. *Journal of Hydrology*, *75*(1–4), 67–110. https://doi.org/10.1016/0022-1694(84)90046-5

Kiel, B. A., & Cardenas, M. B. (2014). Lateral hyporheic exchange throughout the Mississippi River network. *Nature Geoscience*, *7*(6), 413–417. https://doi.org/10.1038/ngeo2157

Kusiak, A., & Song, Z. (2010). Design of wind farm layout for maximum wind energy capture. *Renewable Energy*, *35*(3), 685–694. https://doi.org/10.1016/J.RENENE.2009.08.019

Magliozzi, C., Coro, G., Grabowski, R., Packman, A. I., & Krause, S. (2018). A multiscale statistical method to identify potential areas of hyporheic exchange for river restoration planning. *Environmental Modelling & Software*. https://doi.org/10.1016/J.ENVSOFT.2018.09.006

Mojarrad, B. B., Riml, J., Wörman, A., & Laudon, H. (2019). Fragmentation of the hyporheic zone due to regional groundwater circulation. *Water Resources Research*. https://doi.org/10.1029/2018WR024609

Morén, I., Wörman, A., & Riml, J. (2017). Design of Remediation Actions for Nutrient Mitigation in the Hyporheic Zone. *Water Resources Research*, *53*(11), 8872–8899. https://doi.org/10.1002/2016WR020127

Nikolakopoulou, M., Argerich, A., Drummond, J. D., Gacia, E., Martí, E., Sorolla, A., & Sabater, F. (2018). Emergent Macrophyte Root Architecture Controls Subsurface Solute Transport. *Water Resources Research*, *54*(9), 5958–5972. https://doi.org/10.1029/2017WR022381

Payn, R. A., Gooseff, M. N., McGlynn, B. L., Bencala, K. E., & Wondzell, S. M. (2009). Channel water balance and exchange with subsurface flow along a mountain headwater stream in Montana, United States. *Water Resources Research*, *45*(11). https://doi.org/10.1029/2008WR007644

Pryshlak, T. T., Sawyer, A. H., Stonedahl, S. H., & Soltanian, M. R. (2015). Multiscale hyporheic exchange through strongly heterogeneous sediments. *Water Resources Research*, *51*(11), 9127–9140. https://doi.org/10.1002/2015WR017293

Robinson, N. I., & Love, A. J. (2013). Hidden channels of groundwater flow in Tóthian drainage basins. *Advances in Water Resources*, *62*, 71–78. https://doi.org/10.1016/J.ADVWATRES.2013.10.004

Roche, K. R., Blois, G., Best, J. L., Christensen, K., Aubeneau, A. F., & Packman, A. I. (2018). Turbulence Links Momentum and Solute Exchange in Coarse-Grained Streambeds. *Water Resources Research*. https://doi.org/10.1029/2017WR021992

Schmadel, N. M., Ward, A. S., & Wondzell, S. M. (2017). Hydrologic controls on hyporheic exchange in a headwater mountain stream. *Water Resources Research*, *53*(7), 6260–6278. https://doi.org/10.1002/2017WR020576

Sickbert, T., & Peterson, E. W. (2014). The Effects of Surface Water Velocity on Hyporheic Interchange. *Journal of Water Resource and Protection*, *06*(04), 327–336. https://doi.org/10.4236/jwarp.2014.64035

Stanford, J. A., & Ward, J. V. (1988). The hyporheic habitat of river ecosystems. *Nature*, *335*(6185), 64–66. https://doi.org/10.1038/335064a0

Stonedahl, S. H., Harvey, J. W., Wörman, A., Salehin, M., & Packman, A. I. (2010). A multiscale model for integrating hyporheic exchange from ripples to meanders. *Water Resources Research*, *46*(12). https://doi.org/10.1029/2009WR008865

Stonedahl, S. H., Harvey, J. W., & Packman, A. I. (2013). Interactions between hyporheic flow produced by stream meanders, bars, and dunes. *Water Resources Research*, *49*(9), 5450–5461. https://doi.org/10.1002/wrcr.20400

Storey, R. G., Howard, K. W. F., & Williams, D. D. (2003). Factors controlling riffle-scale hyporheic exchange flows and their seasonal changes in a gaining stream: A three-dimensional groundwater flow model. *Water Resources Research*, *39*(2). https://doi.org/10.1029/2002WR001367

Tonina, D., & Buffington, J. M. (2009). Hyporheic Exchange in Mountain Rivers I: Mechanics and Environmental Effects. *Geography Compass*, *3*(3), 1063–1086. https://doi.org/10.1111/j.1749-8198.2009.00226.x

Tóth, J. (1963). A theoretical analysis of groundwater flow in small drainage basins. *Journal of Geophysical Research*, *68*(16), 4795–4812. https://doi.org/10.1029/JZ068i016p04795

Trauth, M. H. (2015). *MATLAB® recipes for earth sciences, fourth edition*. *MATLAB Recipes for Earth Sciences, Fourth Edition*. https://doi.org/10.1007/978-3-662-46244-7

Vaux, W. G. (1968). Intragravel flow and interchange of water in a streambed. *Fishery Bulletin*, *66*(3), 479–489.

Voltz, T., Gooseff, M., Ward, A. S., Singha, K., Fitzgerald, M., & Wagener, T. (2013). Riparian hydraulic gradient and stream-groundwater exchange dynamics in steep headwater valleys. *Journal of Geophysical Research: Earth Surface*, *118*(2), 953–969. https://doi.org/10.1002/jgrf.20074

Wang, C., Gomez-Velez, J. D., & Wilson, J. L. (2018). The Importance of Capturing

Topographic Features for Modeling Groundwater Flow and Transport in Mountainous Watersheds. *Water Resources Research*, *54*(12), 2018WR023863. https://doi.org/10.1029/2018WR023863

Wang, X.-S., Wan, L., Jiang, X.-W., Li, H., Zhou, Y., Wang, J., & Ji, X. (2017). Identifying three-dimensional nested groundwater flow systems in a Tóthian basin. *Advances in Water Resources*, *108*, 139–156. https://doi.org/10.1016/J.ADVWATRES.2017.07.016

Ward, A. S. (2016). The evolution and state of interdisciplinary hyporheic research. *Wiley Interdisciplinary Reviews: Water*, *3*(1), 83–103. https://doi.org/10.1002/wat2.1120

Ward, A. S., & Packman, A. I. (2019). Advancing our predictive understanding of river corridor exchange. *Wiley Interdisciplinary Reviews: Water*, *6*(1), e1327. https://doi.org/10.1002/wat2.1327

Ward, A. S., Gooseff, M. N., & Johnson, P. A. (2011). How can subsurface modifications to hydraulic conductivity be designed as stream restoration structures? Analysis of Vaux's conceptual models to enhance hyporheic exchange. *Water Resources Research*, *47*(8). https://doi.org/10.1029/2010WR010028

Ward, A. S., Fitzgerald, M., Gooseff, M. N., Voltz, T. J., Binley, A. M., & Singha, K. (2012). Hydrologic and geomorphic controls on hyporheic exchange during base flow recession in a headwater mountain stream. *Water Resources Research*, *48*(4). https://doi.org/10.1029/2011WR011461

Ward, A. S., Gooseff, M. N., Voltz, T. J., Fitzgerald, M., Singha, K., & Zarnetske, J. P. (2013). How does rapidly changing discharge during storm events affect transient storage and channel water balance in a headwater mountain stream? *Water Resources Research*, *49*(9), 5473–5486. https://doi.org/10.1002/wrcr.20434

Ward, A. S., Gooseff, M. N., & Singha, K. (2013). How Does Subsurface Characterization Affect Simulations of Hyporheic Exchange? *Ground Water*, *51*(1), 14–28. https://doi.org/10.1111/j.1745-6584.2012.00911.x

Ward, A. S., Schmadel, N. M., Wondzell, S. M., Gooseff, M. N., & Singha, K. (2017). Dynamic hyporheic and riparian flow path geometry through base flow recession in two headwater mountain streamcorridors. *Water Resources Research*, *53*. https://doi.org/10.1002/2016WR019875

Ward, A. S., Schmadel, N. M., & Wondzell, S. M. (2018a). Simulation of dynamic expansion, contraction, and connectivity in a mountain stream network. *Advances in Water Resources*, *114*, 64–82. https://doi.org/10.1016/J.ADVWATRES.2018.01.018

Ward, A. S., Schmadel, N. M., & Wondzell, S. M. (2018b). Time-Variable Transit Time Distributions in the Hyporheic Zone of a Headwater Mountain Stream. *Water Resources Research*, *54*(3), 2017–2036. https://doi.org/10.1002/2017WR021502

Wlostowski, A. N., Gooseff, M. N., Bowden, W. B., & Wollheim, W. M. (2017). Stream tracer breakthrough curve decomposition into mass fractions: A simple framework to analyze and compare conservative solute transport processes. *Limnology and Oceanography: Methods*, *15*(2), 140–153. https://doi.org/10.1002/lom3.10148

Woessner, W. W. (2000). Stream and Fluvial Plain Ground Water Interactions: Rescaling Hydrogeologic Thought. *Ground Water*, *38*(3), 423–429. https://doi.org/10.1111/j.1745-6584.2000.tb00228.x

Wondzell, S. M. (2006). Effect of morphology and discharge on hyporheic exchange flows in two small streams in the Cascade Mountains of Oregon, USA. *Hydrological Processes*, *20*(2), 267–287. https://doi.org/10.1002/hyp.5902

Wondzell, S. M. (2012). *Hyporheic Zones in Mountain Streams: Physical processes and ecosystem functions*. *Stream Notes. Jan.-Apr. 2012 Issue.* Rocky Mt. Res. Stn., U.S. For. Serv., Fort Collins, CO, U. S. A.

Wondzell, S. M., & Gooseff, M. N. (2013). Geomorphic Controls on Hyporheic Exchange Across Scales: Watersheds to Particles. In *Treatise on Geomorphology*. https://doi.org/10.1016/B978-0-12-374739-6.00238-4

Wondzell, S. M., & Swanson, F. J. (1996). Seasonal and Storm Dynamics of the Hyporheic Zone of a 4th-Order Mountain Stream. I: Hydrologic Processes. *Journal of the North American Benthological Society*, *15*(1), 3–19. https://doi.org/10.2307/1467429

Wondzell, S. M., LaNier, J., & Haggerty, R. (2009). Evaluation of alternative groundwater flow models for simulating hyporheic exchange in a small mountain stream. *Journal of Hydrology*, *364*(1–2), 142–151. https://doi.org/10.1016/J.JHYDROL.2008.10.011

Wörman, A., Packman, A. I., Marklund, L., Harvey, J. W., & Stone, S. H. (2007). Fractal topography and subsurface water flows from fluvial bedforms to the continental shield. *Geophysical Research Letters*, *34*(7), L07402. https://doi.org/10.1029/2007GL029426

Zarnetske, J. P., Haggerty, R., Wondzell, S. M., & Baker, M. A. (2011). Dynamics of nitrate production and removal as a function of residence time in the hyporheic zone. *Journal of Geophysical Research: Biogeosciences*, *116*(G1). https://doi.org/10.1029/2010JG001356

Zimmer, M. A., & Lautz, L. K. (2014). Temporal and spatial response of hyporheic zone geochemistry to a storm event. *Hydrological Processes*, *28*(4), 2324–2337. https://doi.org/10.1002/hyp.9778